99mTc-cAbVCAM1-5 Imaging Is a Sensitive and Reproducible Tool for the Detection of Inflamed Atherosclerotic Lesions in Mice

Alexis Broisat, Jakub Toczek, Laurent Dumas, Mitra Ahmadi, Sandrine Bacot, Pascale Perret, Lotfi Slimani, Gilles Barone-Rochette, Audrey Soubies, Nick Devoogdt, et al.

Title:

^{99m}Tc-cAbVCAM1-5 imaging is a sensitive and reproducible tool for the detection of inflamed atherosclerotic lesions in mouse.

Running foot line:

Sensitivity of ^{99m}Tc-cAbVCAM1-5 imaging

Author's names and affiliations:

Alexis Broisat[1,2*], PhD; Jakub Toczek[1,2*], PhD; Laurent Dumas[1,2], MSc; Mitra Ahmadi[1,2], PhD; Sandrine Bacot[1,2], PhD; Pascale Perret[1,2], PhD; Lotfi Slimani[1,2], PhD;Gilles Barone-Rochette[1,2,3], MD PhD[1]; Audrey Soubies[1,2]; Nick Devoogdt[4], PhD; Tony Lahoutte[4,5], MD PhD; Daniel Fagret[1,2], MD PhD; Laurent M. Riou[1,2], PhD; Catherine Ghezzi[1,2], PhD.

[1]Inserm, U1039, Grenoble, F-38000, France

[2] Université Joseph Fourier Grenoble 1, Radiopharmaceutiques Biocliniques, Grenoble, F-38000, France

[3] Grenoble University Hospital, cardiology department, Grenoble, F-38000, France

[4]In vivo Cellular and Molecular Imaging Laboratory, VrijeUniversiteit Brussel (VUB), Brussels, Belgium

[5]Nuclear Medicine Department, UZ Brussel, Brussels, Belgium

[*] Authors contributed equally

Corresponding and first author:

Alexis Broisat, PhD

Laboratoire des Radiopharmaceutiques Bioclinique

INSERM 1039

Faculté de Médecine de Grenoble

Domaine de la Merci

38700 La Tronche

France

Telephone # +33 4 76 63 71 02

Fax # +33 4 76 63 71 42

Email address: alexis.broisat@inserm.fr

Total Word Count: 4981

Financial support:

This work was partly funded by the French program “Investissementd’Avenir” run by the ‘AgenceNationale pour la Recherche’ ; grant 'Infrastructure d’avenirenBiologie Santé - ANR-11-INBS-0006’ as well as by the ANR-09-TECS-017-01 “PLAQUIMAG” grant.

Abstract

^{99m}Tc-cAbVCAM1-5 is a single-domain antibody fragment (sd-Ab) directed against mouse/human Vascular Cell Adhesion Molecule 1 (VCAM-1) which has recently been proposed as a new imaging agent for the detection of inflamed atherosclerotic lesions. Indeed, in a mouse model of atherosclerosis, ^{99m}Tc-cAbVCAM1-5specifically bound to VCAM-1 positive lesions, thereby allowing their identification on SPECT images. The purpose of the present study was to investigate ^{99m}Tc-cAbVCAM1-5 imaging sensitivity using a reference statin therapy.

Methods. ThirtyApoE-deficient mice were fed a western-type diet. First, the relationship between the level of VCAM-1 expression and ^{99m}Tc-cAbVCAM1-5 uptake was evaluated in 18 mice using immunohistochemistry and autoradiography (ARG). Second, longitudinal SPECT/CT imaging was performed on control (n=9) or atorvastatin-treated mice (0.01% w/w, n=9).

Results.^{99m}Tc-cAbVCAM1-5 uptake in atherosclerotic lesionscorrelated with the level of VCAM-1 expression ($P<0.05$).Atorvastatin exerted significant anti-atherogeniceffects, and ^{99m}Tc-cAbVCAM1-5 lesion uptake was significantly reduced in 35 weeks-old atorvastatin-treated mice, as indicated by ex vivo gamma-well counting and ARG ($p<0.05$). Contrast-CT based SPECT imaging quantification was reproducible (inter experimenter ICC = 0.97, intra experimenter ICC = 0.90), and yielded results that were highly correlated with tracer biodistribution ($r=0.83$; $P<0.0001$). Therefore, reduced ^{99m}Tc-cAbVCAM1-5 uptake in atorvastatin-treated mice was successfully monitored non-invasively by SPECT/CT imaging (0.87 ± 0.06 %ID/cm^3 vs 1.11 ± 0.09 %ID/cm^3 in control group, $P<0.05$).

Conclusions. ^{99m}Tc-cAbVCAM1-5 imaging allowed the specific, sensitive and reproducible quantification of VCAM-1 expression in mice atherosclerotic lesions. ^{99m}Tc-cAbVCAM1-5 therefore exhibits suitable characteristics for the evaluation of novel anti-atherogenic agents..

Keywords: ^{99m}Tc-cAbVCAM1-5, Atherosclerosis, VCAM-1, Molecular Imaging

Introduction.

Atherosclerosis constitutes a worldwide health challenge*(1)*. Despite major advances in imaging technologies*(2)*, a major need for imaging probes targeting vulnerable plaques (VP) still exists. Such a tool could be used for diagnosis and prognosis as well as for the monitoring of treatment efficacy*(3)*. A major criterion for the identification of VP is inflammation*(4)*. Vascular cell adhesion molecule 1 (VCAM-1) plays a major role in the infiltration of inflammatory cells into atherosclerotic lesions (*5)*. Indeed, in human atherosclerotic lesions, VCAM1 expression was observed at the level of the luminal endothelium as well as on neovessels, macrophages and activated smooth muscle cells of advanced lesions*(5–7)*. Therefore, the assessment of VCAM-1 expression levels in atherosclerotic plaques could potentially be highly relevant in order to identify prone-to-rupture lesions *(8)*. Due to the small size and location of VP, imaging agents with optimal characteristics are required. Single domain antibody (sdAb)-derived radiotracers, that have originally been developed in the field of oncology*(9)*, have recently been proposed by our group as a new class of imaging agents with optimal characteristics for cardiovascular imaging*(10)*and the radiolabelled anti-VCAM-1 camel antibody fragment^{99m}Tc-cAbVCAM1-5 compound was selected among 10 VCAM-1-specific sdAbas the most potent candidate. Accordingly, aortic plaques were successfully visualized non-invasively by single photon emission computed tomography (SPECT) in an Apolipoprotein E (ApoE) deficient mouse model of atherosclerosis, with binding specificity being further demonstrated by *in vivo* competition experiments. Importantly, the production and selection processes of VCAM-1 sdAbwere specifically designed to produce cross-reactive,murine & human binders. The nanomolar affinity of^{99m}Tc-cAbVCAM1-5 for both human and murine VCAM-1 therefore makes the tracerpotentially suitable for clinical translation*(10)*.

The main objective of the present study was to investigate the sensitivity of ^{99m}Tc-cAbVCAM1-5 for the imaging of VCAM-1 expression in murine atherosclerotic lesions.

Indeed, high sensitivity is a key requirement for VP imaging as well as for the preclinical assessment of the efficacy of novel anti-atherogenic therapies. In accordance with the major role of inflammatory processes in the development of VP, the anti-inflammatory effect of new therapeutic agents targeting at the lipid profile such as cholesteriylesterasetransfert protein inhibitors is currently being investigated*(11)*. In addition, therapeutic interventions aimed at directly targeting the inflammatory process are also under evaluation*(3)* using drugs such as methotrexate, canakinumab or losmapimod*(12–14)*. A specific and sensitive imaging agent targeting at the inflammatory process occurring in atherosclerotic lesions would therefore be of great relevance for the evaluation of novel anti-atherogenic agents.

Statins are well established and widely used therapeutics in clinical practice, and atorvastatin has previously been employed for the evaluation of new imaging agents in mouse models of atherosclerosis*(15–17)*.In the present preclinical study, atorvastatin was used in order to evaluate the potential of ^{99m}Tc-cAbVCAM1-5for the monitoring of treatment efficacy in ApoE deficient mice.

Methods

Animal model

All experimental procedures werein accordance with institutional guidelines and approved by the Animal Care & Use committee (ComEth) of the University ofGrenoble.

Twelve (12) 40-wks old female ApoE-deficient mice (Charles River) fed a western type diet were used for the ex vivo comparison between ^{99m}Tc-cAbVCAM1-5 uptake in atherosclerotic lesions and VCAM-1 expression.

Eighteen female ApoE-deficient mice were used for the non invasive evaluation of a reference therapy.At the age of 15 weeks, mice were either fed a western diet (control group, n=9) or a western diet supplemented with a reference therapy (0.01% atorvastatin) (treated group, n=9). In these two groups, average food consumption and animal weight were

assessed weekly and blood sampling was performed before and 10 weeks following the onset of western diet for total cholesterol determination (BioMerieux). The effect of the statin therapy on ^{99m}Tc-cAbVCAM1-5 uptake in atherosclerotic lesions was evaluated in vivo using longitudinal SPECT/CT imaging on 25 and 35 weeks-old mice, and ex vivo by gamma well counting (GWC) and autoradiography.

Radiolabeling.

cAbVCAM1-5 labeling with ^{99m}Tc was performed as previously described*(10)*. Briefly, [^{99m}Tc(H_20)$_3$(CO)$_3$]$^+$ (^{99m}Tc-tricarbonyl) was synthesized by adding 1 mL of $^{99m}TcO_4^-$ solution to an Isolink kit (PSI). The vial was incubated at 100°C for 20 min and neutralized with HCl. Then, 0.5mL of ^{99m}Tc-tricarbonyl was added to 50 µg of cAbVCAM1-5 and 50 µl of 50mM carbonate buffer pH 8.0, and this mixture was incubated for 90 min at 50°C. The ^{99m}Tc-cAbVCAM1-5 solution was further gelfiltrated on Sephadex G25 (NAP-5; GE Healthcare) and filtered (0.22 µm Millex, Millipore). Radiochemical purity, determined by RP-HPLC, was >95% up to 6h following radiolabelling.

^{99m}Tc-cAbVCAM1-5 uptake versus VCAM-1 expression. ^{99m}Tc-cAbVCAM1-5 uptake in atherosclerotic lesions and VCAM-1 expression level were determined using autoradiographicimagingand immunohistochemistry , respectively (n=12). Three (3) hours following intraveinousinjection of 37±3MBq (mean±SD), mice were euthanized using CO_2. The aortic arch was cleaned in 10% formalin (Sigma) under a binocular (Discovery V8, Zeiss), embedded in optimal cutting temperature (OCT) medium and frozen in -40°Cisopentane. Serial 20µm or 8µm-thick adjacent slices were obtained for Autoradiography and immunohistochemistry, respectively (HM 505E, Microm).For the purpose of this study, longitudinal orientation was preferred for it allowed simultaneous examination of several lesions, located in the ascending aorta, small curvature of the aortic arch, innominate, left common carotid and left subclavian arteries, and descending aorta.

Autoradiography

Autoradiographieswere acquiredusing overnight exposure with a phosphor-Imager (BAS-5000, Fujifilm). All slices were then stained using standard hematoxylin-eosin-safrantrichrome staining (HES), digitalized, andHES and autoradiographicimages were coregistered using GIMP2 and ImageJsoftwares. Regions of interest (ROIs) were drawn on atherosclerotic lesions based on HES staining. Internal references with known amounts of radioactivity were used to express tracer activity as percent injected dose per gram (%ID/g)following background and decay correction.

Immunohistochemistry

VCAM-1 immunostaining(sc-1504, santa-Cruz) was performedas previously described*(10)*onslices adjacent to those used for autoradiography / HES. VCAM-1 expression level in atherosclerotic lesions (n=94) was ranked as low, moderate or strong by a trained observer blinded to the autoradiographicimages. This analysis was reproduced 2 months later by the same observer in order to assess the reproducibility of themethodology.

Non invasive evaluation of a reference therapy.

SPECT/CT imaging

SPECT/CT acquisitions were performed two hours following an intravenous injection of 55±5 MBq(mean±SD) of ^{99m}Tc-cAbVCAM1-5.The mice were anesthetized using isoflurane 1.5% in a 1:1 mixture of room air and oxygen, and then placed in a temperature-controlled bed for SPECT/CT acquisitions focused on the thoracic region (nanoSPECT, Bioscan). First, the helicoidal SPECT acquisition was performed with 4 heads equipped with multi-pinholes collimators (9 x 1.4 mm diameter pinhole per head) using 24 projections and 45 min of acquisition. Then, a fast, 1.5min-long CT acquisition was performed immediately following retro-orbital injection of 150µl of a vascular contrast agent (Hexabrix), using the following

acquisition parameters: 65kvp, 180 projections and 500ms per projection. Contrast-CT and SPECT acquisitions were reconstructed fused and quantified using dedicated software (InVivoScope).

SPECT/CT quantification

Contrast-CT based SPECT quantification was performed blinded to the SPECT images. Briefly, 4 Volumes of Interest (VOIs) of 2.2mm^{3}each were drawn at the level of the aortic sinus and ascending aorta based on contrast-CT images. ^{99m}Tc-cAbVCAM1-5 activity was expressed as apercent injected dose per cube centimeter (%ID/cm^3) and uptake in atherosclerotic lesions was defined as the maximumvalue fromquantification of 4 VOIs. Moreover, in order to assess the inter and intra-observer variability, 35 weeks SPECT images were further quantified by 3 additional independent experimenters, and this quantification was reproduced 2 weeks later by one of the experimenters.

Ex vivo quantification

Following SPECT/CT imaging, anesthetized mice were euthanized using CO_2 and ascending aortas including the aortic sinus were carefully harvested along with major organs. Tissue samples were weighed and their activity was determined by GWC (Wizard^2, Perkin). The results were corrected for background and decay and expressed as a percent of injected dose per gram of tissue (%ID/g). Adjacent transversal 40- and 10µm-thick cryosections were obtained at the level of the aortic sinus for autoradiographicimaging and immunostaining, respectively, and autoradiography quantification was performed following HES staining as described above. ROIs were also used to determine lesion area in mm^2. ^{99m}Tc-cAbVCAM1-5 uptake was expressed as a %ID per gram of lesion (“concentration”) based on internal references.Alternatively, lesion volumein the analyzed slice was determined as the product between its surface and the slice thickness (40µm), and ^{99m}Tc-cAbVCAM1-5 uptake was then expressed as a %ID present in the analyzed slice (“total uptake”).

Statistical analysis.

All results are presented as mean±s.e.m. F-test was employed for variances comparisons. Student t, Mann &Witney U, Pearson,intraclass coefficient (ICC) and Kappa tests were employed forpaired/unpaired datasets with equal variances, unpaired datasets with unequal variances,correlation analysis,and inter/intra experimenters variability, respectively. Differences were considered significant for P<0.05.

Results

^{99m}Tc-cAbVCAM1-5 uptake versus VCAM-1 expression.

Heterogeneous VCAM-1 expression levels were observed following immunostainingof longitudinal slices from the aortic arch of Apo-deficient mice (figure 1A&C). VCAM-1 was expressed by endothelial as well as intra-plaque cells. Intra-observer ranking of VCAM-1 expression level was found to be reproducible (kappa=0.70). Robust ^{99m}Tc-cAbVCAM1-5 uptake was observed following autoradiographicimaging of VCAM-1 positive lesions (figure 1B&D). Autoradiographyquantification confirmed the relationship between ^{99m}Tc-cAbVCAM1-5 uptake and the level of VCAM-1 expression (figure 1E). Indeed, a graded tracer uptakeof 1.4 ± 0.2, 2.5 ± 0.2 and 3. 2 ± 0.3 %ID/g was observed in low, moderate and strong VCAM-1 expressing lesions, respectively (*P*<0.001 between low and moderate or strong, and *P* = 0.029 between moderate and high).

Non invasive evaluation of a reference therapy

Lesion extension.

The results are presented in Table 1 and Figure 1. Similar cholesterol levels were observed between treated and control animals prior to switching from chow to western dietcontaining (treated) or not (control) atorvastatin (20.3±2.2 *vs* 18.8±2.2 mmol/L, P = NS). Average atorvastatin intake was 12.9±0.2 mg/kg/day/animal and resulted in a significant 29.1%

decrease in total cholesterol level in the atorvastatin-treated group in comparison with the control group (60.7±6.6 vs 85.5±8.1 mmol/L; *P* = 0.034). Lesion extension in the aortic sinus was significantly reduced by 39.9% in the treated group in comparison to that of the control group (0.70 ± 0.07 *vs* 1.07 ± 0.11 mm^2, *P* = 0.011) (Table 1 and suppl. fig. 1). Finally, modest variations in VCAM-1 expression in the aortic sinus were observed between control and treated animals following immunohistochemistry(suppl. fig. 1).

In vivo SPECT/CT imaging.

^{99m}Tc-cAbVCAM1-5 allowed the non-invasive monitoring of atorvastatin effect on atherosclerosis. Indeed, ^{99m}Tc-cAbVCAM1-5 uptake in aortic lesions was readily visible on SPECT images (figure 2) and the trend towards a reduction of ^{99m}Tc-cAbVCAM1-5 uptake that was observed in 25 weeks-old atorvastatin-treated mice (0.83 ± 0.09 %ID/cm^3 *vs* 0.97 ± 0.06 %ID/cm^3 in control group, P=NS) reached statistical significance at 35 weeks (0.87 ± 0.06 %ID/cm^3 *vs* 1.11 ± 0.09 %ID/cm^3 in control group, *P* = 0.035). Contrast-CT acquisitions allowed the accurate delineation of the ascending aorta in all animals, and contrast-CT based SPECT quantification was reproducible, with inter- and intra- experimenter ICC of 0.97 and 0.90, respectively (Figure 3).

Ex vivo gamma-well counting.

^{99m}Tc-cAbVCAM1-5 biodistribution is presented in Table 2. ^{99m}Tc-cAbVCAM1-5 uptake in atorvastatin-treated animals was significantly decreased by 24.1 % in the ascending aorta of atorvastatin-treated animals (0.9 ± 0.1 *vs* 1.2 ± 0.1 %ID/g, *P* = 0.015). The tracer was mainly eliminated through the kidneys (138.7 ± 8.6 %ID/g) with minimal uptake in all other investigated tissues (< 2 %ID/g) with the exception of lymphoid organs. Indeed, tracer uptake in the spleen, thymus, bone marrow and lymph node was of 8.8 ± 0.7; 2.1 ± 0.2; 4.0 ± 0.4 and 2.8 ± 0.3 %ID/g, respectively.

Exvivo autoradiography.

In both groups, robust ^{99m}Tc-cAbVCAM1-5 uptake in atherosclerotic lesions was readily observable at the level of the aortic sinus (suppl. fig. 1 A-D). A strong and statistically significant 41.5% decrease in ^{99m}Tc-cAbVCAM1 total uptake was observed in the atorvastatin-treated group in comparison to that of the control group (table 3). Indeed ^{99m}Tc-cAbVCAM1 uptake represented $8.9x10^{-5} \pm 1.1x10^{-5}$%ID/slice in the control group and $5.2\ 10^{-5} \pm 0.9\ 10^{-5}$ %ID/slice in the treated group. Interestingly,autoradiography quantification indicated a trend toward a 15.2% decrease of ^{99m}Tc-cAbVCAM1-5 concentration in atherosclerotic lesions from atorvastatin-treated animalswhen tracer uptake was corrected for plaque area (1.8 ± 0.2 %ID/g *vs* 2.1 ± 0.2 %ID/g in control group, P=NS),

Comparison between SPECT/CT, autoradiography, and gamma-well counting data

Further data analysis indicated that SPECT/CT quantification was strongly correlated to ex vivo gamma-well counting biodistribution (r = 0.83; P<0.0001) (figure 4A). Moreover, the results from SPECT/CT image quantification were significantly correlated to ^{99m}Tc-cAbVCAM1 total uptake in aortic sinus lesions as determined by autoradiography (r = 0.51; P = 0.04), rather than to ^{99m}Tc-cAbVCAM1 concentration or to lesion area (P=NS for both) (figure 4 B-D).

Discussion

Atorvastatin significantly reduced lesion extension in the aortic sinus of ApoE-deficient mice, and this effect was successfully monitored non-invasively using ^{99m}Tc-cAbVCAM1-5 molecular imaging with high reproducibility. ^{99m}Tc-cAbVCAM1-5 is therefore a specific, sensitive and reproducible tool for the imaging of VCAM-1 expression in murine atherosclerotic lesions.

Effect of statin therapy.The anti-atherosclerotic effects of statins are mainly mediated by their cholesterol-lowering properties leading to reduced plaque volume*(18)*. In addition,

statins also exert pleiotropic effects which go beyond the drop in plasma cholesterol and which mainly result in an inhibition of inflammatory processes responsible for vulnerable plaque development*(19,20)*. However, depending on the dose &duration of the treatment and on study design, the reduction in plasma cholesterol, plaque volume and inflammatory markers are not always consistently or concomitantly observed in experimental studies. Indeed, in an ApoE-deficient mouse model of carotid artery lesions induced by perivascular collar placement, Bot and coll. observed that a low dose of atorvastatin (0.003%w/w) significantly reduced lesion size by 40% despite no reduction in total plasma cholesterol or macrophage positive areas*(15)*. Conversely, a twelve week atorvastatin treatment (1 mg/kg/day) resulted in a significant reduction in the circulating inflammatory markers Interleukin-6 and Monocyte Chemoattractant Protein-1 as well as macrophage infiltration in aortic lesions of apoE-deficientmice despite no significant change in plasma cholesterol and plaque area*(21)*.

The western-type diet-fed apoE-deficient mice that were used in the present study had a mean total blood cholesterol level of 85.5±8.1 mmol/L, in good accordance with the 28-114 mmol/L range reported on a similar model by Nakashima and coll*(22)*. Supplementation of the western-type diet with 0.01% w/w atorvastatin resulted in an expected administered dose of ≈10mg/kg/day*(16)*. Atorvastatin significantly decreased total cholesterol by 29% and lesion size by 40%. These results are in accordance with the range of atorvastatin-induced modifications reported by other groups*(16,17)*. Modest changes in the lesional expression of VCAM-1 were observed in atorvastatin-treated animals, in contrast with other studies showing a significant 30-80% reduction in VCAM-1 expression*(16,17,23)*. However, Nachtigal and coll found no significant change in VCAM-1 lesion expression in double knock-out, $LDLR^{-/-}ApoE^{-/-}$ mice in the presence of atorvastatin at a similar dose to that used in the present study*(24)*.

Overall, atorvastatin administered at a dose of 0.01% w/w for 20 weeks to ApoE-deficient mice fed a western-type diet therefore had significant anti-atherogenic effects that allowed the evaluation of the potential of ^{99m}Tc-cAbVCAM1-5 for treatment effect monitoring.

Sensitivity of ^{99m}Tc-cAbVCAM1-5 imaging.

^{99m}Tc-cAbVCAM1-5 uptake occurred in atherosclerotic lesions as well as in lymphoid organs constitutively expressing VCAM-1 following tracer injection to ApoE-deficient mice fed a western type diet, in accordance with previously published results*(10)*. Autoradiography and immunohistochemistryindicatedthat^{99m}Tc-cAbVCAM1-5 uptake in atherosclerotic lesion significantly increased together with the level of VCAM-1 expression. Importantly, ^{99m}Tc-cAbVCAM1-5lesion uptake was significantly reduced in 35 weeks-old atorvastatin-treated mice as indicated by ex vivo GWC and autoradiography as well as in vivonon invasiveSPECT/CT molecular imaging. In vivo image quantification was reproducible and yielded results that were highly correlated withtracer biodistributionas determined ex vivo.

More precisely, VOIsfrom in vivo images were reproducibly drawn at the level of the aortic sinus based on contrast-CT images. In the hypothesis that the VOI exclusively contained atherosclerotic lesional tissues and according to the fact that ^{99m}Tc-cAbVCAM1-5 uptake in murine atherosclerotic lesion significantly increased together with the level of VCAM-1 expression, SPECT quantification would then have directly reflected the levelof VCAM-1 expression in atherosclerotic lesions. However, due to the relatively small size of atherosclerotic lesions, and despite the use of a state-of-the-art, sub-millimetric resolution system, partial volume effect necessarily occurred while performing SPECT imaging of murine aortic plaques. Therefore, the VOI used for the assessment of tracer uptake in atherosclerotic lesions contained a mixture of the various tissues composing the aortic sinus – i.e. atherosclerotic lesions, normal vessel wall and blood – rather than the atherosclerotic lesion only. Consequently, the total activity in a VOI, and therefore the result of *in vivo* quantification, depended not only upon the level of VCAM-1expression in the lesions but also

upon the amount of lesions included in the VOI, and therefore lesion extension. This was demonstrated in the present study by the fact that the results from SPECT/CT image quantification were significantly correlated to ^{99m}Tc-cAbVCAM1 total uptake in aortic sinus lesions as defined by the product of ^{99m}Tc-cAbVCAM1 concentration in lesion by lesion volume – rather than with any one of these two parameters considered separately.In conclusion, ^{99m}Tc-cAbVCAM1-5 SPECT/CT imaging allowed the sensitive and reproducible non-invasive quantification of the net effect of a reference statin therapy on lesion size and inflammation in the apoE-deficient mouse model of atherosclerosis.

Comparison with other radiotracers and molecular targets.

The sensitivity of ^{99m}Tc-cAbVCAM1-5 imaging favorably compared with previously evaluated radiotracers. In a rabbit model of atherosclerosis,Haider and coll. observed a decrease in the uptake of two SPECT agents directed against matrix metalloproteinases(MPI) and apoptosis (AA5)followingtreatment with fluvastatin*(25)*.Although SPECT image quantification was not performed,thesequalitative visual observations were further confirmed by quantitative ex vivo analysis. Similarly, a significant 30% reduction in^{18}F-4V was found by in vivo positron emission tomography(PET)image quantification in a similar model to that employed in the present study*(23)*. A number of studies have investigated the potential of ^{18}F-FDG for the non-invasive assessment of treatment efficacy. Such potentialhas been validated in rabbits using the anti-oxydantprobucol*(26)*, thereby allowing the use of ^{18}F-FDGfor the evaluation of novel therapeutics in preclinical*(27,28)* and clinical studies*(12,29)*. However, high myocardial uptake remains a potential limitation for the imaging of coronary lesions with ^{18}F-FDGdespite the use of imaging protocols aimed at reducing myocardial tracer uptake*(30)*.

VCAM-1 protein is strongly and specifically expressed during the inflammatory process, and therefore constitutes a highly relevant target for VP imaging, similarly to other inflammatory markers such as macrophages. Other biological processes related to plaque rupture such as apoptosis, matrix degradation or neoangiogenesis*(31)* have been proposed as potential targets. These processes occur at different times and intraplaque locations over the course

of plaque development. Ultimately, prospective clinical trials will be needed in order to select the most appropriate target and corresponding imaging agent.

Conclusions

SdAbsderived radiotracers have been initially developed in the field of oncology, and a first phase I clinical trial is currently been performed with an anti-human epidermal growth factor receptor 2radiotacer for PET imaging of breast cancer patients. Thereafter, anti-VCAM-1 sdAb extended the field of sdAb imaging to cardiovascular applications. As demonstrated in the present study, ^{99m}Tc-cAbVCAM1-5 is a sensitive tool for the non-invasive imaging of atherosclerosis. Indeed, ^{99m}Tc-cAbVCAM1-5 uptake in mouse atherosclerotic lesions was correlated to the level of VCAM-1 expression, and the effect of a reference therapy was successfully and reproducibly monitored non-invasively by SPECT/CT imaging quantification. ^{99m}Tc-cAbVCAM1-5 therefore exhibits suitable characteristics for evaluation of novel anti-atherogenic agents.

Disclosures: none

Acknowledgments:

Antony Coradin, Pierre-Francois Meyer and AudreyGenoud, students of Grenoble University, were involved in data collection and analysis during their training course in RadiopharmaceutiquesBiocliniques Laboratory. This work was partly funded by the French program “Investissementd’Avenir” run by the ‘AgenceNationale pour la Recherche’ ; grant 'Infrastructure d’avenirenBiologie Santé - ANR-11-INBS-0006’ as well as by the ANR-09-TECS-017-01 “PLAQUIMAG” grant.

References

1. Sanz J, Moreno PR, Fuster V. The year in atherothrombosis.J Am CollCardiol. 2013;62:1131–1143.

2. Libby P, DiCarli M, Weissleder R. The vascular biology of atherosclerosis and imaging targets.J Nucl Med. 2010;51Suppl 1:33S–37S.

3. Berman JP, Farkouh ME, Rosenson RS. Emerging anti-inflammatory drugs for atherosclerosis.Expert OpinEmerg Drugs. 2013;18:193–205.

4. Fuster V, Moreno PR, Fayad ZA, Corti R, Badimon JJ. Atherothrombosis and high-risk plaque: part I: evolving concepts. J Am CollCardiol. 2005;46:937–954.

5. O'Brien KD, McDonald TO, Chait A, Allen MD, Alpers CE. Neovascular expression of E-selectin, intercellular adhesion molecule-1, and vascular cell adhesion molecule-1 in human atherosclerosis and their relation to intimal leukocyte content.Circulation. 1996;93:672–682.

6. O'Brien KD, Allen MD, McDonald TO, et al. Vascular cell adhesion molecule-1 is expressed in human coronary atherosclerotic plaques. Implications for the mode of progression of advanced coronary atherosclerosis.J Clin Invest. 1993;92:945–951.

7. Davies MJ, Gordon JL, Gearing AJ, et al. The expression of the adhesion molecules ICAM-1, VCAM-1, PECAM, and E-selectin in human atherosclerosis.J Pathol. 1993;171:223–229.

8. Naghavi M, Libby P, Falk E, et al. From vulnerable plaque to vulnerable patient: a call for new definitions and risk assessment strategies: Part II. Circulation. 2003;108:1772–1778.

9. Xavier C, Vaneycken I, D'huyvetter M, et al. Synthesis, preclinical validation, dosimetry, and toxicity of 68Ga-NOTA-anti-HER2 Nanobodies for iPET imaging of HER2 receptor expression in cancer. J Nucl Med. 2013;54:776–784.

10. Broisat A, Hernot S, Toczek J, et al. Nanobodies targeting mouse/human VCAM1 for the nuclear imaging of atherosclerotic lesions. Circ Res. 2012;110:927–937.

11. Barter PJ, Rye K-A. Cholesteryl ester transfer protein inhibition as a strategy to reduce cardiovascular risk. J Lipid Res. 2012;53:1755–1766.

12. Elkhawad M, Rudd JHF, Sarov-Blat L, et al. Effects of p38 mitogen-activated protein kinase inhibition on vascular and systemic inflammation in patients with atherosclerosis. JACC Cardiovasc Imaging. 2012;5:911–922.

13. Everett BM, Pradhan AD, Solomon DH, et al. Rationale and design of the Cardiovascular Inflammation Reduction Trial: a test of the inflammatory hypothesis of atherothrombosis. Am Heart J. 2013;166:199–207.e15.

14. Ridker PM, Thuren T, Zalewski A, Libby P. Interleukin-1β inhibition and the prevention of recurrent cardiovascular events: rationale and design of the Canakinumab Anti-inflammatory Thrombosis Outcomes Study (CANTOS). Am Heart J. 2011;162:597–605.

15. Bot I, Jukema JW, Lankhuizen IM, van Berkel TJC, Biessen EAL. Atorvastatin inhibits plaque development and adventitial neovascularization in ApoE deficient mice independent of plasma cholesterol levels. Atherosclerosis. 2011;214:295–300.

16. Khanicheh E, Mitterhuber M, Xu L, Haeuselmann SP, Kuster GM, Kaufmann BA. Noninvasive ultrasound molecular imaging of the effect of statins on endothelial inflammatory phenotype in early atherosclerosis.PLoS ONE. 2013;8:e58761.

17. Nahrendorf M, Jaffer FA, Kelly KA, et al. Noninvasive vascular cell adhesion molecule-1 imaging identifies inflammatory activation of cells in atherosclerosis. Circulation. 2006;114:1504–1511.

18. Brautbar A, Ballantyne CM. Pharmacological strategies for lowering LDL cholesterol: statins and beyond. Nat Rev Cardiol. 2011;8:253–265.

19. Rasmussen LM, Hansen PR, Nabipour MT, Olesen P, Kristiansen MT, Ledet T. Diverse effects of inhibition of 3-hydroxy-3-methylglutaryl-CoA reductase on the expression of VCAM-1 and E-selectin in endothelial cells. Biochem J. 2001;360:363–370.

20. Ridker PM, Danielson E, Fonseca FAH, et al. Rosuvastatin to prevent vascular events in men and women with elevated C-reactive protein. N Engl J Med. 2008;359:2195–2207.

21. Grothusen C, Bley S, Selle T et al. Combined effects of HMG-CoA-reductase inhibition and renin-angiotensin system blockade on experimental atherosclerosis. Atherosclerosis. 2005;182:57–69.

22. Nakashima Y, Plump AS, Raines EW, Breslow JL, Ross R. ApoE-deficient mice develop lesions of all phases of atherosclerosis throughout the arterial tree. ArteriosclerThromb. 1994;14:133–140.

23. Nahrendorf M, Keliher E, Panizzi P, et al. 18F-4V for PET-CT imaging of VCAM-1 expression in atherosclerosis. JACC Cardiovasc Imaging. 2009;2:1213–1222.

24. Nachtigal P, Pospisilova N, Jamborova G et al. Atorvastatin has hypolipidemic and anti-inflammatory effects in apoE/LDL receptor-double-knockout mice. Life Sci. 2008;82(13-14):708-17.

25. Haider N, Hartung D, Fujimoto S, et al. Dual molecular imaging for targeting metalloproteinase activity and apoptosis in atherosclerosis: molecular imaging facilitates understanding of pathogenesis. J NuclCardiol. 2009;16:753–762.

26. Ogawa M, Magata Y, Kato T, et al. Application of 18F-FDG PET for monitoring the therapeutic effect of antiinflammatory drugs on stabilization of vulnerable atherosclerotic plaques.J Nucl Med. 2006;47:1845–1850.

27. Vucic E, Dickson SD, Calcagno C, et al. Pioglitazone modulates vascular inflammation in atherosclerotic rabbits noninvasive assessment with FDG-PET-CT and dynamic contrast-enhanced MR imaging. JACC Cardiovasc Imaging. 2011;4:1100–1109.

28. Vucic E, Calcagno C, Dickson SD, et al. Regression of inflammation in atherosclerosis by the LXR agonist R211945: a noninvasive assessment and comparison with atorvastatin. JACC Cardiovasc Imaging. 2012;5:819–828.

29. Tawakol A, Fayad ZA, Mogg R, et al. Intensification of statin therapy results in a rapid reduction in atherosclerotic inflammation: results of a multicenter fluorodeoxyglucose-positron emission tomography/computed tomography feasibility study. J Am CollCardiol. 2013;62:909–917.

30. Harisankar CNB, Mittal BR, Agrawal KL, Abrar ML, Bhattacharya A. Utility of high fat and low carbohydrate diet in suppressing myocardial FDG uptake.J NuclCardiol. 2011;18:926–936.

31. Sadeghi MM, Glover DK, Lanza GM, Fayad ZA, Johnson LL. Imaging atherosclerosis and vulnerable plaque. J Nucl Med. 2010;51Suppl 1:51S-65S.

Figure Legends

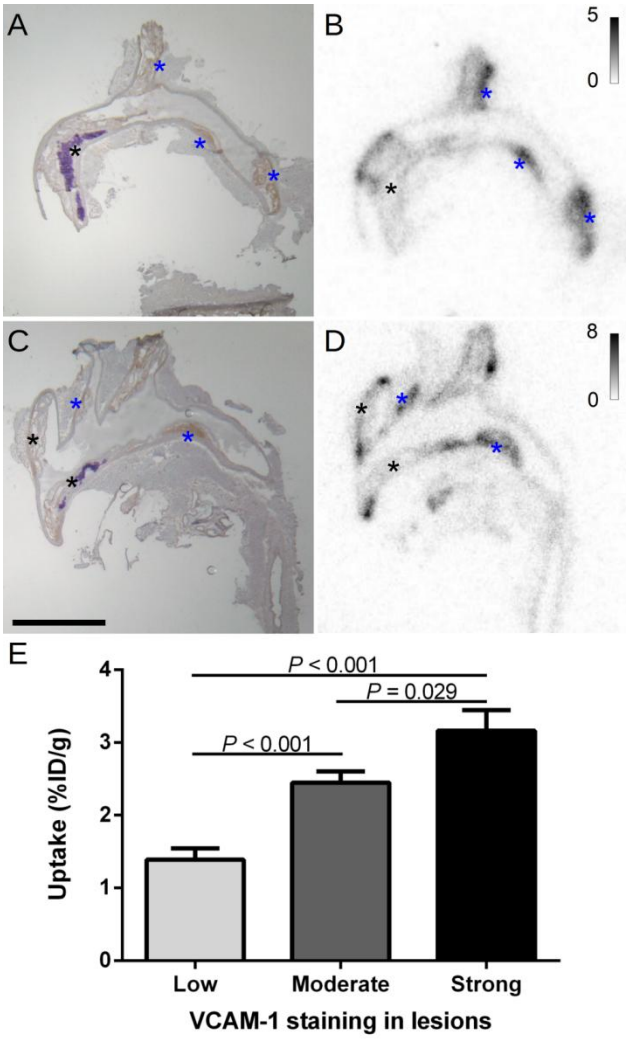

FIGURE 1.^{99m}Tc-cAbVCAM1-5 uptake and VCAM-1 expression. A and C: Representative VCAM-1 immunostainings performed on aortic arch lesions of ApoE-deficient mice. B and D: ^{99m}Tc-cAbVCAM1-5 ARG imaging performed on adjacent slices. Strong ^{99m}Tc-cAbVCAM1-5 uptake was observed on atherosclerotic lesions expressing high level of VCAM-1 (blue asterisks), in comparison to atherosclerotic lesions expressing low levels of VCAM-1 (black asterisks). This result was further confirmed by autoradiography quantification (E). Scale bar: 500µm; Autoradiography calibration bar is expressed in %ID/g.

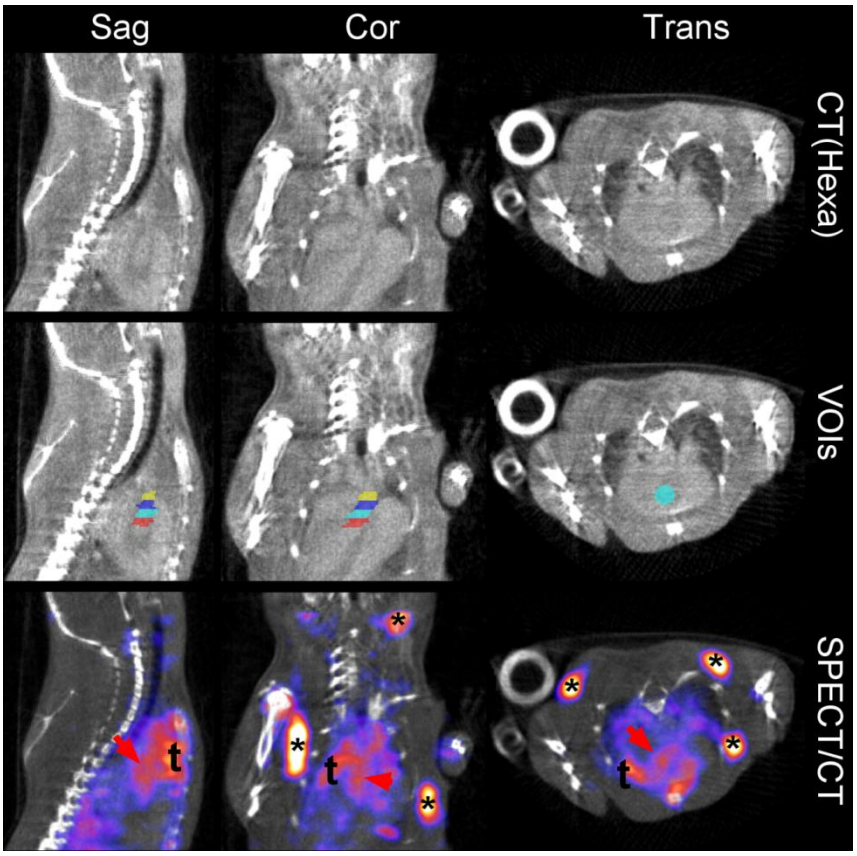

FIGURE2.In-vivo SPECT/CT imaging. Representative example of sagittal (1st column), coronal (2nd column) and transaxial (3rd column) views centered on the ascending aorta of control group mouse are presented here. Myocardial cavities and major vessels including the aorta were easily identifiable on contrast-CT images (1st row), allowing to precisely defining four VOIs along the aortic sinus and ascending aorta (2nd row).^{99m}Tc-cAbVCAM1-5 uptake was readily visible by SPECT within the aorta (red arrow), as well as in tissues constitutively expressing VCAM-1 such as the lymph nodes (asterisks) and thymus (t). SPECT scale was normalized from 0.3 to 3%ID/cm^3.

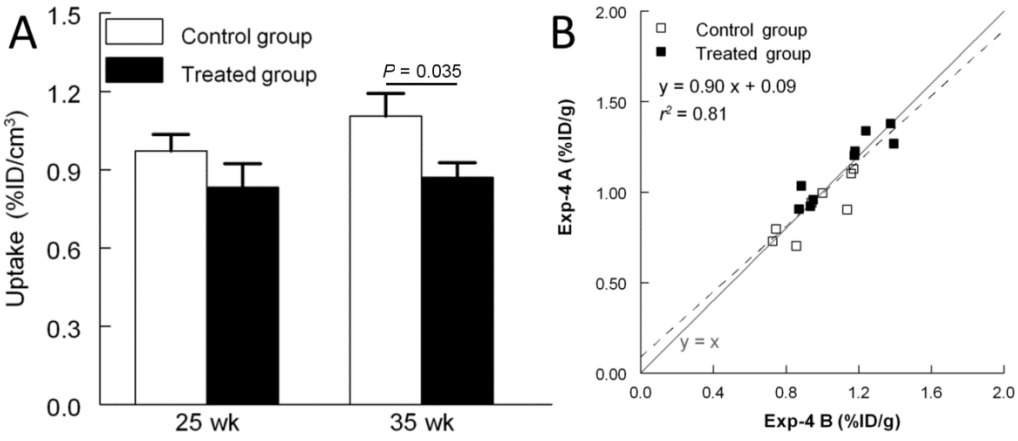

C

	Exp 1	Exp 2	Exp 3	Exp 4-A	Exp4-B
Control (%ID/cm³)	1.11 ± 0.09	1.16 ± 0.08	1.14 ± 0.08	1.14 ± 0.06	1.13 ± 0.07
Treated (%ID/cm³)	0.87 ± 0.06	0.93 ± 0.05	0.97 ± 0.05	0.94 ± 0.06	0.97 ± 0.06
Inter Exp		ICC = 0.97			-
Intra Exp	-	-	-	ICC = 0.90	

FIGURE3.SPECT/CT quantification. The reduction of ^{99m}Tc-cAbVCAM1-5 uptake in treated mice aorta was successfully monitored *in vivo* by SPECT/CT imaging (A). Furthermore, contrast-CT based SPECT analysis provided robust quantifications, as determined by intra-experimenter correlation (B) and inter/intra experimenter ICCs (C).

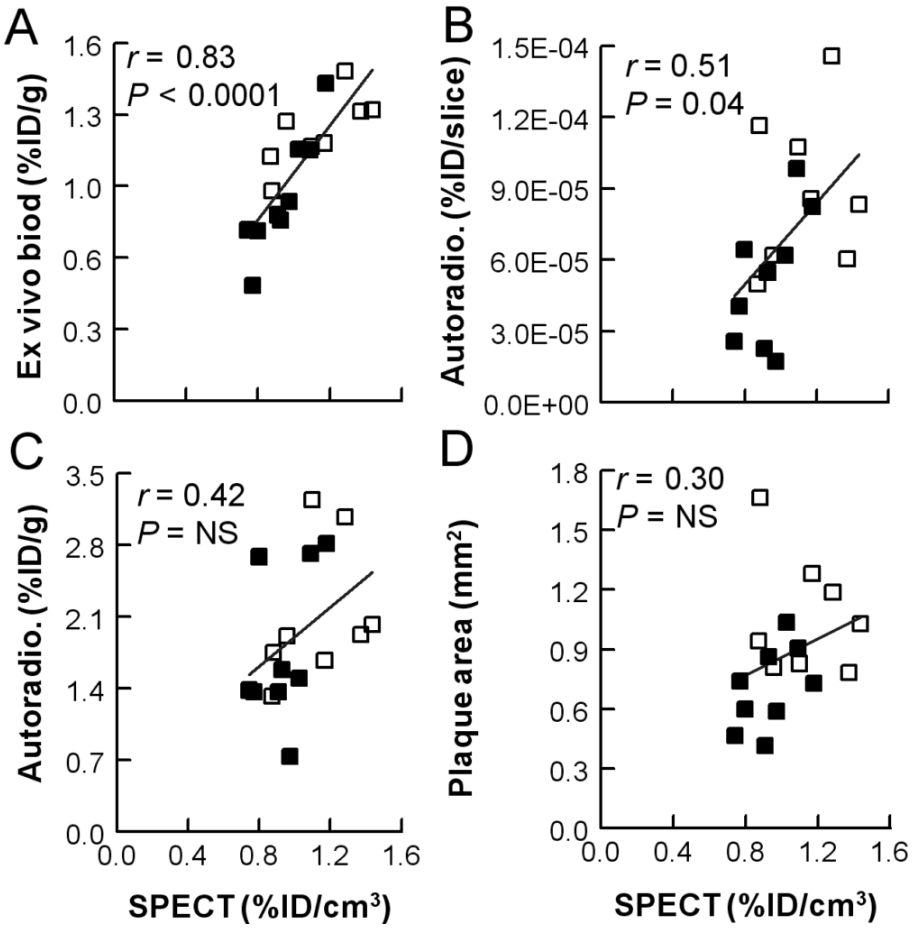

FIGURE4.Comparison between *in vivo* and ex *vivo* quantifications of ^{99m}Tc-cAbVCAM1-5 uptake in atherosclerotic lesions.SPECT/CT quantification was compared to ex vivo biodistribution in samples constituted of the aortic sinus and ascending aorta (A), as well as to the autoradiography quantification results either expressed as a total uptake in lesions per slice (B) or as a concentration (C), and to plaque area (D).White markers: Control group. Black markers: Treated group.

Tables

Parameter		Unit	control	treated	% change
Tot. Cho.	Chow diet	mmol/L	20.3±2.2	18.8±2.2	NS
	Western diet	mmol/L	85.5±8.1	60.7±6.6	- 29.1 (*P* = 0.034)
Lesion area		mm^2	1.07±0.11	0.70±0.07	- 33.9 (*P* = 0.011)

TABLE 1.Effect of treatment on lesions extension.Atorvastatin 0.01% significantly decreased total plasma cholesterol as well as lesion extension at the level of the aortic sinus.

	Control	Treated
As. Aorta	1.2±0.1	0.9±0.1*
Blood	0.6±0.1	0.5±0.0
Heart	0.3±0.0	0.3±0.0
Lung	1.7±0.1	1.8±0.1
Liver	1.5±0.1	1.4±0.1
SM	0.1±0.0	0.3±0.1
SG	0.7±0.2	0.7±0.1
Thyroid	1.2±0.2	0.9±0.2
Stomach	0.7±0.1	0.7±0.1
Bile	0.4±0.0	0.5±0.1
Kidney	138.7±8.6	165.0±6.8
Spleen	8.8±0.7	7.9±0.5
Thymus	2.1±0.2	1.8±0.2
BM	4.0±0.4	4.1±0.7
LN	2.8±0.3	2.7±0.2

TABLE 2.*Ex vivo* biodistribution of ^{99m}Tc- cAbVCAM1-5 3h post-injection in ApoE-deficient mice. Results are expressed as %ID/g (mean ± s.e.m.). * *P* =0.015 vs control group. SM, skeletal muscle; SG, salivary glands; BM, bone marrow; LN, lymph node.

Parameter	Unit	Control	Treated	% change
Total uptake	%ID/slice (.10^{-6})	8.9 ± 1.2	5.2 ± 0.9	- 41.5 (*P*=0.024)
Concentration	%ID/g	2.1 ± 0.2	1.8 ± 0.2	NS

TABLE 3.Ex vivo autoradiography quantification on the aortic sinus lesions.Atorvastatin therapy resulted in a statistically significant decrease in ^{99m}Tc-cAbVCAM1 total uptake in atherosclerotic lesions. Furthermore, there was also a trend toward a 15.2% decrease of ^{99m}Tc-cAbVCAM1-5 concentration in atorvastatin-treated group when tracer uptake was corrected for plaque area (*P* = NS)